ISSN: 0975-833X

Available online at http://www.journalcra.com

International Journal of Current Research
Vol. 10, Issue, 11, pp.75477-75489, November, 2018
DOI: https://doi.org/10.24941/ijcr.33257.11.2018

INTERNATIONAL JOURNAL OF CURRENT RESEARCH

RESEARCH ARTICLE

PREDICTION AND OPTIMIZATION OF HEAT INPUT ON MILD STEEL WELDMENTS

***Atalor, N.D., Achebo, J.I. and Osarenmwinda J.O.**

Department of Production Engineering, University of Benin, Benin City, Nigeria

ARTICLE INFO

Article History:
Received 24th August, 2018
Received in revised form
27th September, 2018
Accepted 29th October, 2018
Published online 30th November, 2018

Key Words:
Heat Input,
RSM and lack of fit.

ABSTRACT

Excessive weld penetration is a weld defect that affects weld quality and the service life of Engineering Structures, such defects can be eliminated by the optimum selection of welding process parameters. This study is carried out to optimize the heat input, An experimental matrix was developed with the design expert software, which resulted in a composite design. Mild steel plate of 10mm thickness was cut to size measuring 80mm in length and 40mm in width, the samples were grinded, polished and welded with the Tungsten Inert Gas. Thereafter the heat input was determined for the weld samples, the experimental results was used as the data. The Response Surface Methodology, was employed to optimize the responses from input parameters which includes current, voltage and gas flow rate. The experimental results shows that the minimum value for current is 120, voltage 20, gas flow rate 12 and the maximum value are 170 Amp, 25 volt, 14Lit/mm. The RSM model selected the quadratic model as the suitable model for the heat input, deposition rate, weld penetration size because it has a p – value < 0.05. The models developed possessed good noise to signal ratio of 9.47 for heat input. The optimal numerical solution was obtained and the result shows that a current of 157.67 will combine with 24.44 volt and 12.34 Lit/min to produce a weld having 0.603 heat input.

Citation: Atalor, N.D, Achebo, J.I and Osarenmwinda J.O., 2018. "Prediction and optimization of heat input on mild steel weldments", *International Journal of Current Research*, 10, (11), 75477-75489.

INTRODUCTION

The amount of energy introduced into a weld during any arc welding process, is regarded as the "heat input". It is a critical parameter that should be considered and controlled to make sure weld quality meet the required standard. Popovic *et al.*, (2010) reported that the welding heat input has a great influence on the thermal and mechanical properties of welded structures. The heat input plays a vital role of governing the cooling rates in welds and thereby causing a change in the microstructural configuration on the weld metal toughness. The cross sectional area of a weld is generally proportional to the amount of heat input. As more energy is supplied to the arc, more filler material and base metal will be melted per unit length, resulting in a larger weld bead. The quality of the welded material can be evaluated by many characteristics, such as penetration size, bead width, bead height and deposition rate Deshmukh *et al.*, (2014). These characteristics are controlled by a number of welding parameters and therefore to attain good quality, it is important to set up the proper welding process parameters. But the underlying mechanism connecting the welding parameters and quality characteristics is usually not known.

Corresponding author: **Atalor, N.D.,**
Department of Production Engineering, University of Benin, Benin City, Nigeria

Kim and Rhee (2001) mentioned that there are several other experimental designs that can be used such as astagucchi, full factorial and genetic algorithm but are faced with some limitations. They also stated that as the number of inputs increases the number of experiment increases exponentially making the full factorial design inefficient which requires the modification of the experimental design space. Apurv and Vijaykumar(2014) investigates the effect of heat input (controlled by welding current, welding voltage and welding speed) on tensile strength, micro-hardness and microstructure of austenitic 202 grade stainless steel weldments produced by shielded metal arc welding (SMAW). The base material used in the present investigation was Cr-Mn SS and 308L SS solid electrode was used as the filler material. From the experimental results, it was found that the increase in heat input affects the micro-constituents of base metal, and heat affected zone (HAZ). Tensile strength decreases with increase in heat input and from scanning electron microscopy of tensile test fractured surfaces exhibited ductile & brittle failure. From micro hardness data values it was observed that hardness of material increases with increase in heat input in weld pool and decreases in HAZ zone. Optical microscopy shows that smaller dendrite sizes and lesser inter-dendritic spacing were observed in the fusion zone at low heat input. And long dendrite sizes and large inter-dendritic spacing were observed in the fusion zone of the joint welded at high heat input. Further it was observed from the optical micrographs that the extent of grain

coarsening in the HAZ increases with increase in heat input. Hari and Sunil, (2013) shows the effect of heat input on dilution and how it affects the heat affected zone in submerged arc welding process, they concluded that excessive heat inputs greatly increases the heat affected zone. Hu *et al.* (2013), and Honggang *et al.* (2014), also proved from their article that excessive heat input greatly alters the microstructural properties of the metal. The relationship can be developed by using experimental design techniques. According to Myers and Montgomery (1995), the experimental optimization of any welding process is often a very costly and time consuming task, due to many kinds of non-linear events involved. One of the most widely used methods to solve this problem is the Response Surface Methodology (RSM) Suneel and Jagadeesh (2016), Correia *et al.*, (2005) and Doniavi *et al.*, (2016). In this method, the experimenter tries to approximate the unknown mechanism with an appropriate empirical model, being the function that it represents which is called a response surface model. Identifying and fitting from experimental data a good response surface model requires some knowledge of statistical experimental design fundamentals, regression modeling techniques and elementary optimization methods.

MATERIALS AND METHODS

Materials: 100 pieces of mild steel coupons measuring 80 x 40 x10mm was used for the experiments, the experiment was performed 20 times, using 5 specimens for each run.100% pure Argon gas was used in this research study. The key parameters considered in this work are welding current, welding speed, gas flow rate and welding voltage.

The range of the process parameters obtained from literature is shown in the table 1.The tungsten inert gas welding equipment was used to produce the weld specimen after the edges have been machined. Figure 1 shows the TIG welding setup.

Table 1. Process parameters and their levels

Process parameters	Unit	Symbol	Low (-)	High (+)
Welding Current	Amp	I	120	170
Welding Voltage	Volts	V	20	25
Gas Flow Rate	Lit/mill	F	12	14

Table 2. Experimental Matrix (CCD) in actual factors

Runs	I (A)	V	GFR (L/min)
1	170	20	12
2	170	20	12
3	170	25	14
4	170	25	14
5	120	25	14
6	170	21	14
7	120	22	12
8	130	20	14
9	130	22	12
10	120	22	14
11	120	20	14
12	140	23	12
13	140	24	12
14	140	22	14
15	120	23	12
16	120	25	12
17	150	20	12
18	150	22	12
19	140	21	14
20	170	23	14

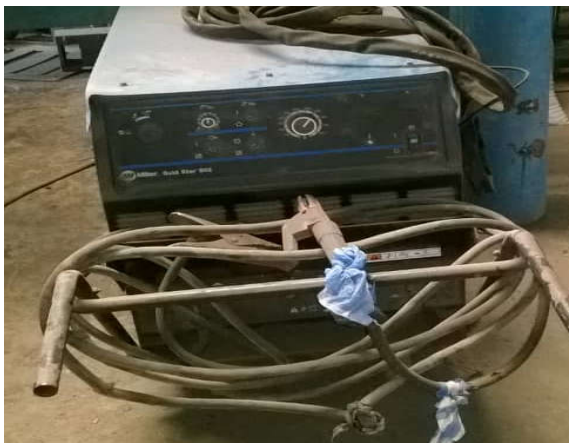

Figure 1. TIG equipment

Figure 3. Shielding gas cylinder and regulator

Fig. 2. TIG Torch

Fig. 4. Tungsten electrode

The welding process uses a shielding gas to protect the weld specimen from atmospheric interaction, a weld torch directs the gas to the region of weld. Figure 2 and Figure3 shows the weld torch and shielding gas cylinder and regulator.In this experiment, the dimension used for the TIG welding electrode is 1.6 – 3.2 and 4mm. this was chosen on the basis of the current intensity. The electrode is shown in the Figure 4.

Central Composite Design

A second-order model can be constructed efficiently with central composite designs (CCD) (Montgomery, 1997). CCDs are first-order (2 N) designs augmented by additional centre and axial points to allow estimation of the tuning parameters of a second-order model. Figure 5 shows CCD for 3 design variables.

Table 3. Table of output Parameters, Units and Symbols

S/N	Responses	Notations	Unit
1	Deposition Rate	DR	Kg/minute
2	Weld penetration	WP	mm
3	Heat Input	HI	KJ/minute

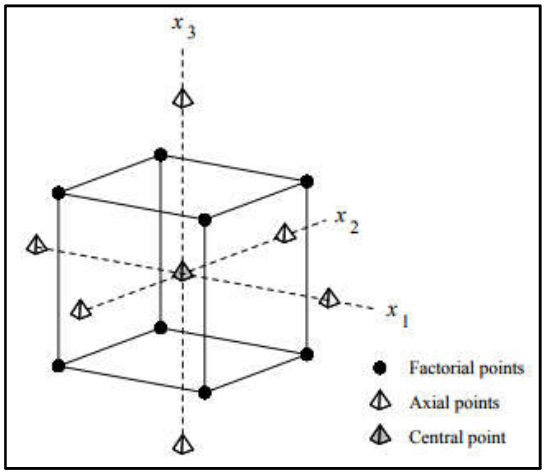

Figure 5. Central Composite Design for 3 Design Variables at 2 Levels

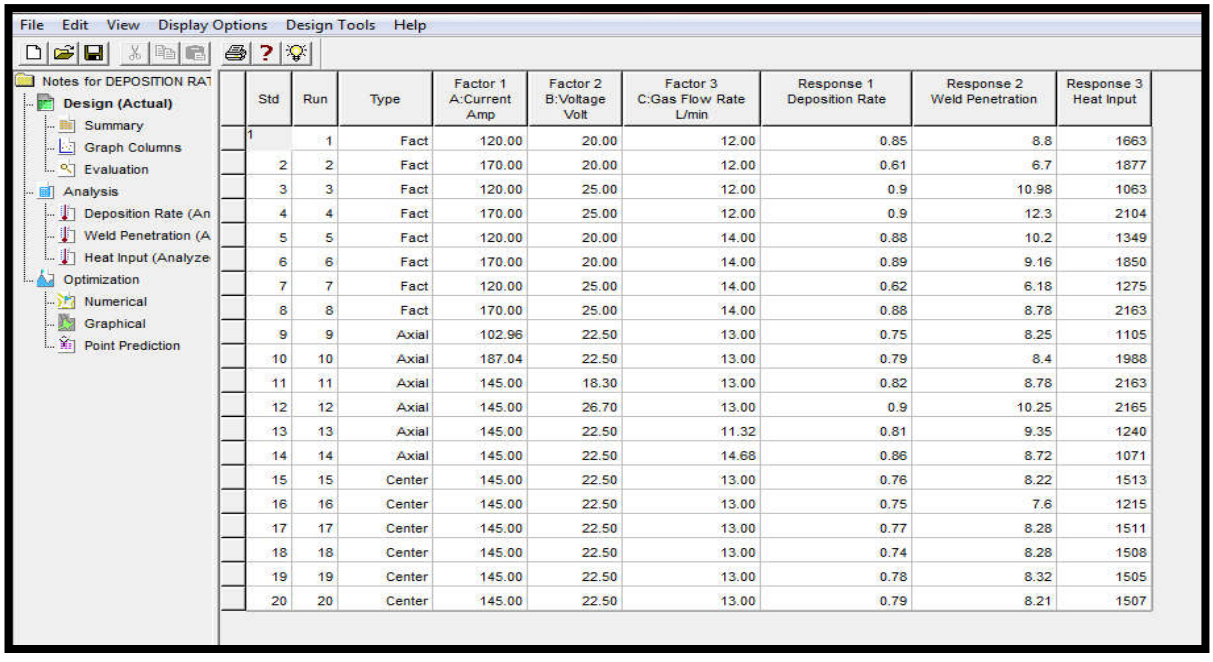

Std	Run	Type	Factor 1 A:Current Amp	Factor 2 B:Voltage Volt	Factor 3 C:Gas Flow Rate L/min	Response 1 Deposition Rate	Response 2 Weld Penetration	Response 3 Heat Input
1	1	Fact	120.00	20.00	12.00	0.85	8.8	1663
2	2	Fact	170.00	20.00	12.00	0.61	6.7	1877
3	3	Fact	120.00	25.00	12.00	0.9	10.98	1063
4	4	Fact	170.00	25.00	12.00	0.9	12.3	2104
5	5	Fact	120.00	20.00	14.00	0.88	10.2	1349
6	6	Fact	170.00	20.00	14.00	0.89	9.16	1850
7	7	Fact	120.00	25.00	14.00	0.62	6.18	1275
8	8	Fact	170.00	25.00	14.00	0.88	8.78	2163
9	9	Axial	102.96	22.50	13.00	0.75	8.25	1105
10	10	Axial	187.04	22.50	13.00	0.79	8.4	1988
11	11	Axial	145.00	18.30	13.00	0.82	8.78	2163
12	12	Axial	145.00	26.70	13.00	0.9	10.25	2165
13	13	Axial	145.00	22.50	11.32	0.81	9.35	1240
14	14	Axial	145.00	22.50	14.68	0.86	8.72	1071
15	15	Center	145.00	22.50	13.00	0.76	8.22	1513
16	16	Center	145.00	22.50	13.00	0.75	7.6	1215
17	17	Center	145.00	22.50	13.00	0.77	8.28	1511
18	18	Center	145.00	22.50	13.00	0.74	8.28	1508
19	19	Center	145.00	22.50	13.00	0.78	8.32	1505
20	20	Center	145.00	22.50	13.00	0.79	8.21	1507

Figure 6. Design matrix showing the real values and the experimental values

Method of Data Collection

The central composite design matrix was developed using the design expert software, producing 20 experimental runs. The input parameters and output parameters make up the experimental matrix and the responses recorded from the weld samples was used as the data. The table below shows the central composite design matrix.

In Figure 5, the design involves 2 N factorial points, 2N axial points and 1 central point. CCD presents an alternative to 3N designs in the construction of second-order models because the number of experiments is reduced as compared to a full factorial design (15 in the case of CCD compared to 27 for a full-factorial design). The CCD was adopted for this research due to its flexibility with respect to the issue of 2 way interactions.

RESULTS AND DISCUSSION

RESULTS

The randomized design matrix comprising of three input variables namely; current (Amp), voltage (Volt) and gas flow rate (l/min) and three response variable (heat input) in real values is presented in Figures 6. The model summary which shows the factors and their lowest and highest values including the mean and standard deviation is presented as shown in figure 7 which revealed that the model is of the quadratic type which requires the polynomial analysis order as depicted by a typical response surface design.

The minimum value of deposition rate was observed to be 0.610g/s, with a maximum value of 0.90g/s, mean value of 0.802 and standard deviation of 0.083.For weld penetration, the minimum value was observed to be 6.180mm, with a maximum value of 12.30mm, mean value of 8.788 and standard deviation of 1.344.For heat input, the minimum value was observed to be 1063J/mm, with a maximum value of 2165J/mm, mean value of 1591.75 and standard deviation of 374.224. To validate the suitability of the quadratic model in analyzing the experimental data, the sequential model sum of squares was calculated for the heat input as presented in Figure 8. The sequential model sum of squares table shows the accumulating improvement in the model fit as terms are added.

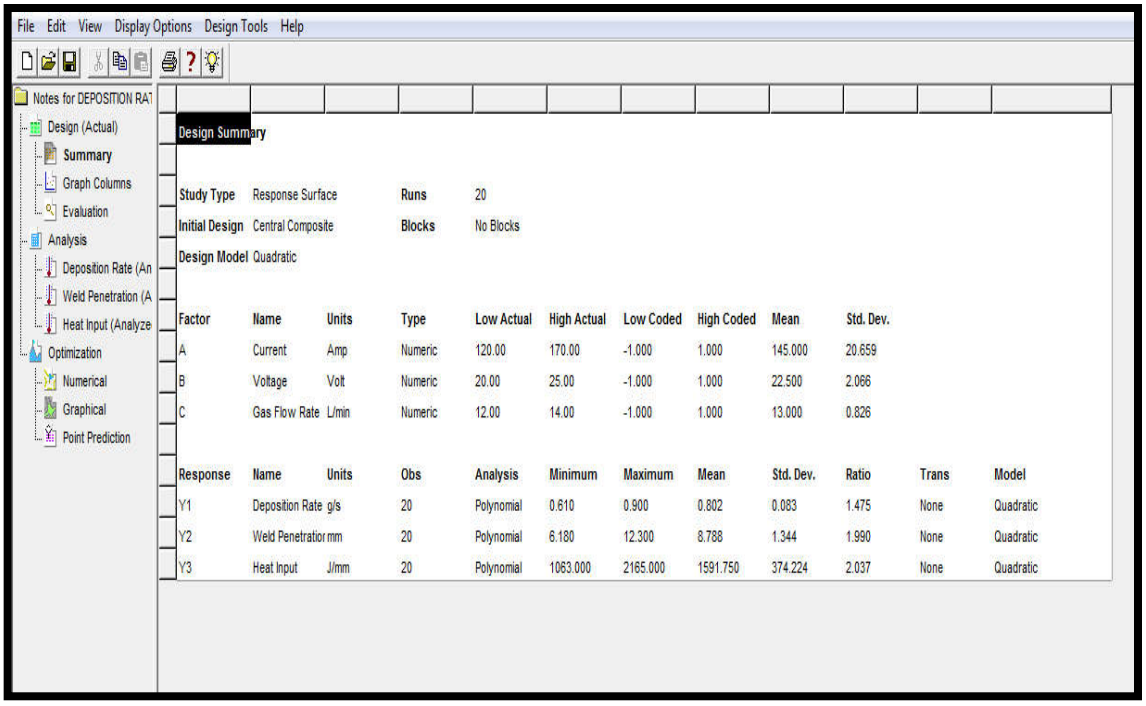

Figure 7. RSM design summary

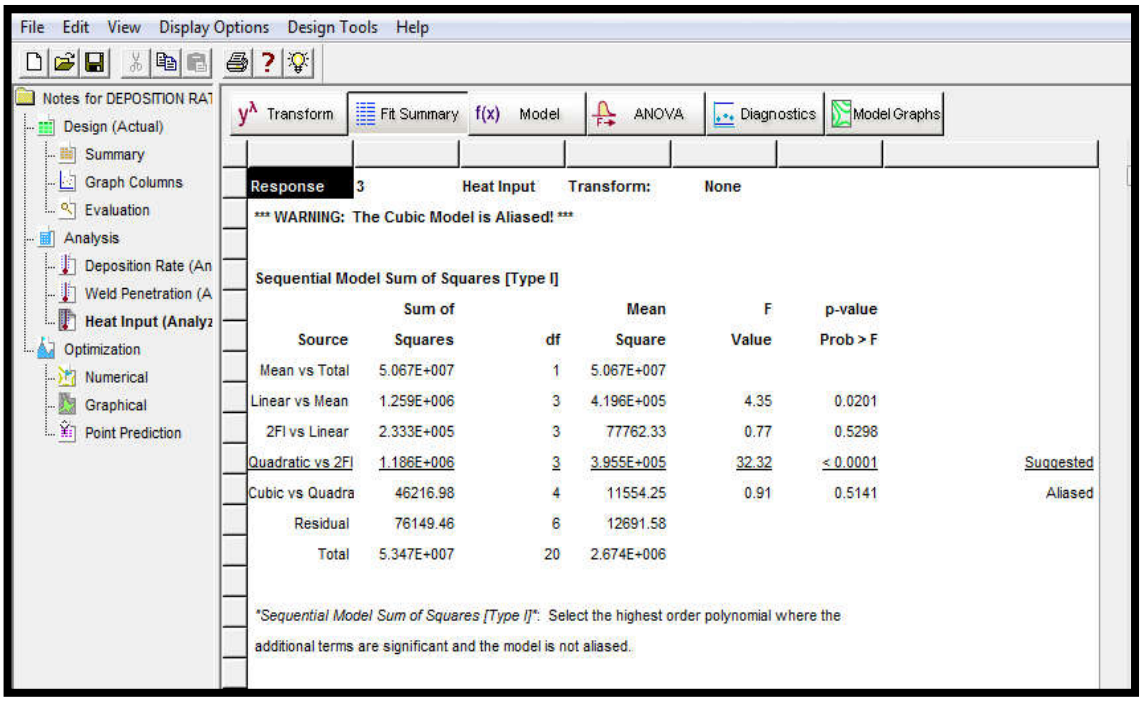

Figure 8. Sequential model sum of square for heat input

Based on the calculated sequential model sum of square, the highest order polynomial where the additional terms are significant and the model is not aliased was selected as the best fit. From the result of figure 8, it was observed that the cubic polynomial was aliased hence cannot be employed to fit the final model. In addition, the quadratic and 2FI model were suggesed as the best fit thus justifying the use of quadratic polynomial in this analysis. To test how well the quadratic model can explain the underlying variation associated with the experimental data, the lack of fit test was estimated for each of the responses. Model with significant lack of fit cannot be employed for prediction. Results of the computed lack of fit for the heat input is presented in Figure 9.

predicted error sum of square (PRESS) statistic for each complete model. Low standard deviation, R-Squarednear one and relatively low PRESS is the optimum criteria for defining the best model source. Based on the results of figure10 the quadratic polynomial model was suggested while the cubic polynomial model was aliased hence, the quadratic polynomial model was selected for this analysis. Analysis of the model standard error was employed to assess the suitability of response surface methodology using the quadratic model to maximize the deposition rate, weld penetration and optimize the heat input. The computed standard errors for the selected responses is presented in Figure 11. From the results of Table 11, it was observed that the model possess a low standard error

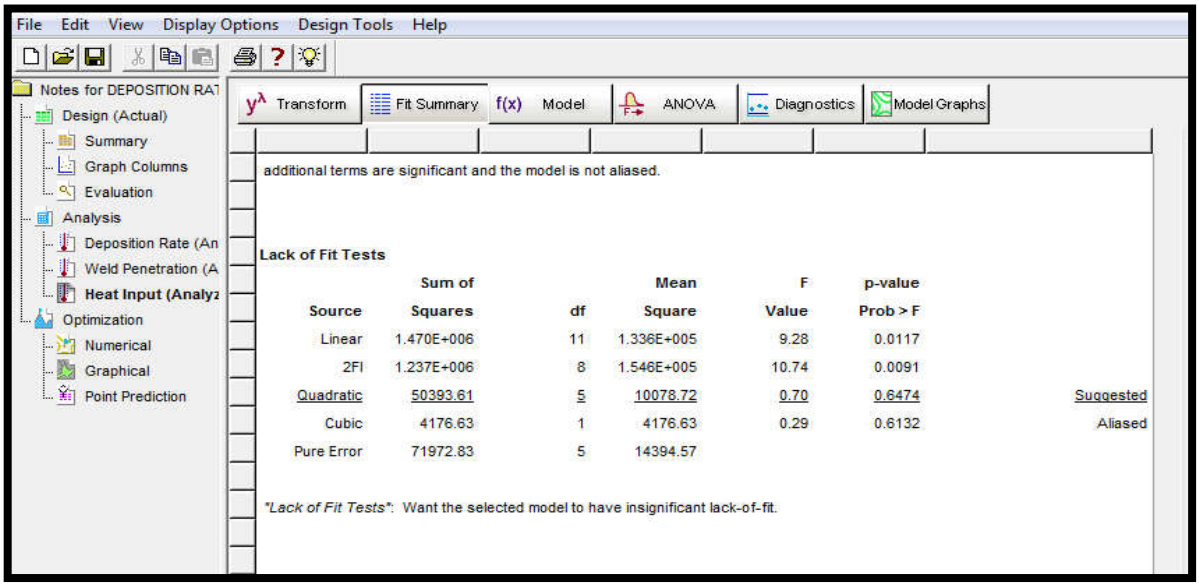

Figure 9. Lack of fit test for heat input

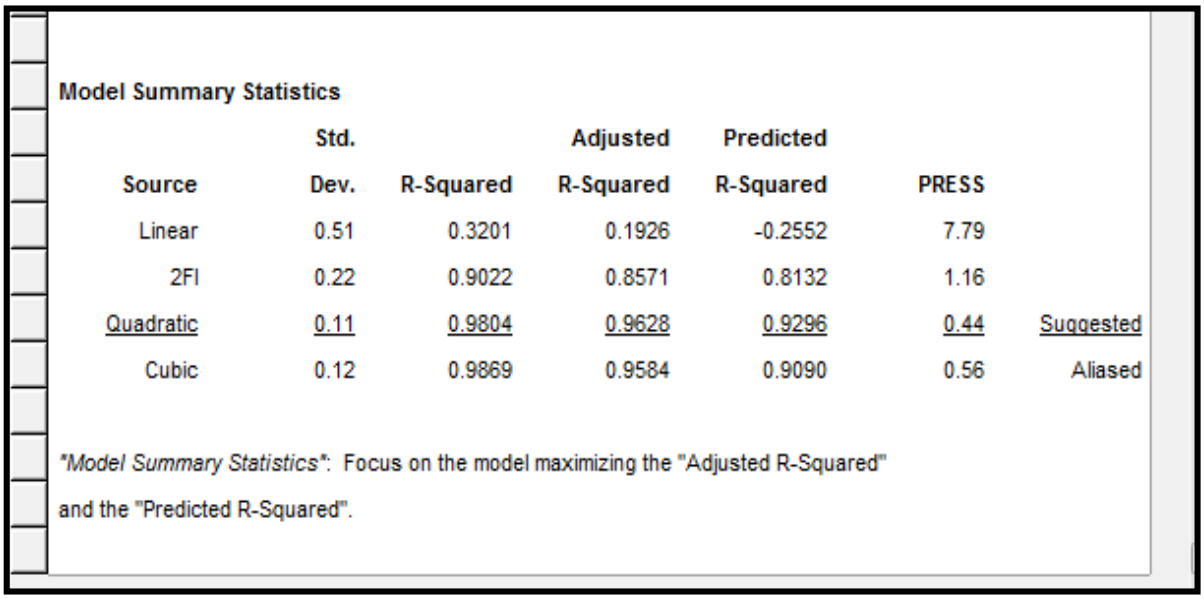

Figure 10. Model summary statistics for heat input

From the result of figure 9, it was again observed that the quadratic polynomial had a non-significant lack of fit and was suggest for model analysis while the cubic polynomial had a significand lack of fit hence aliased to model analysis. The model statistics computed for heat input response based on the different model sources is presented in Figure 10. The summary statistics of model fit shows the standard deviation, the r-squared, adjusted r-squared, predicted r-squared and

ranging from 0.27 for the individual terms, 0.35 for the combine effects and 0.26 for the quadratic terms. Standard errors should be similar within type of coefficient; smaller is better. The error values were also observed to be less than the model basic standard deviation of 1.0 which suggests that response surface methodology was ideal for the optimization process. The correlation matrix of regression coefficient is presented in Figure 12.

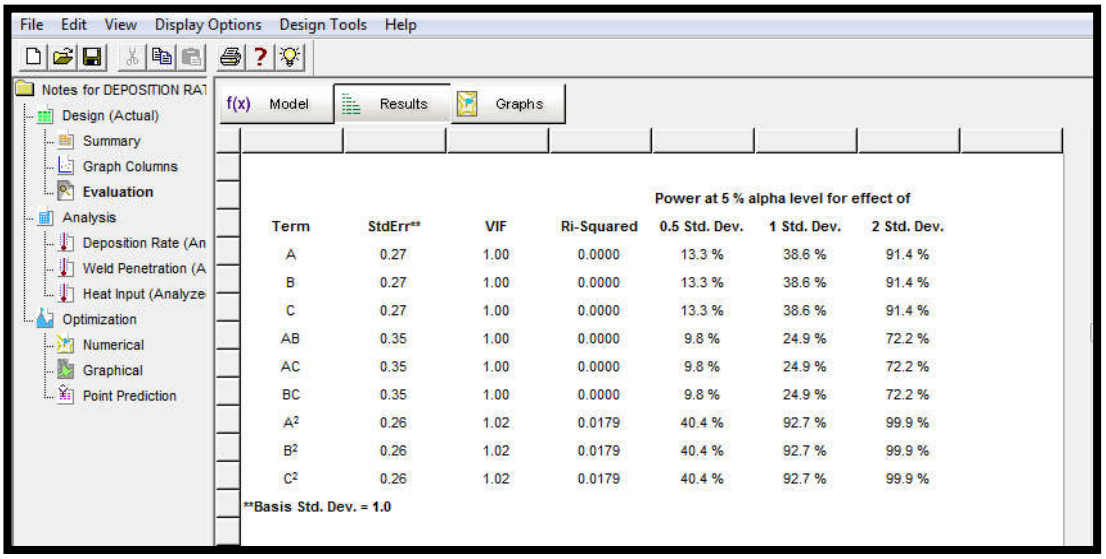

Figure 11. Result of computed standard errors

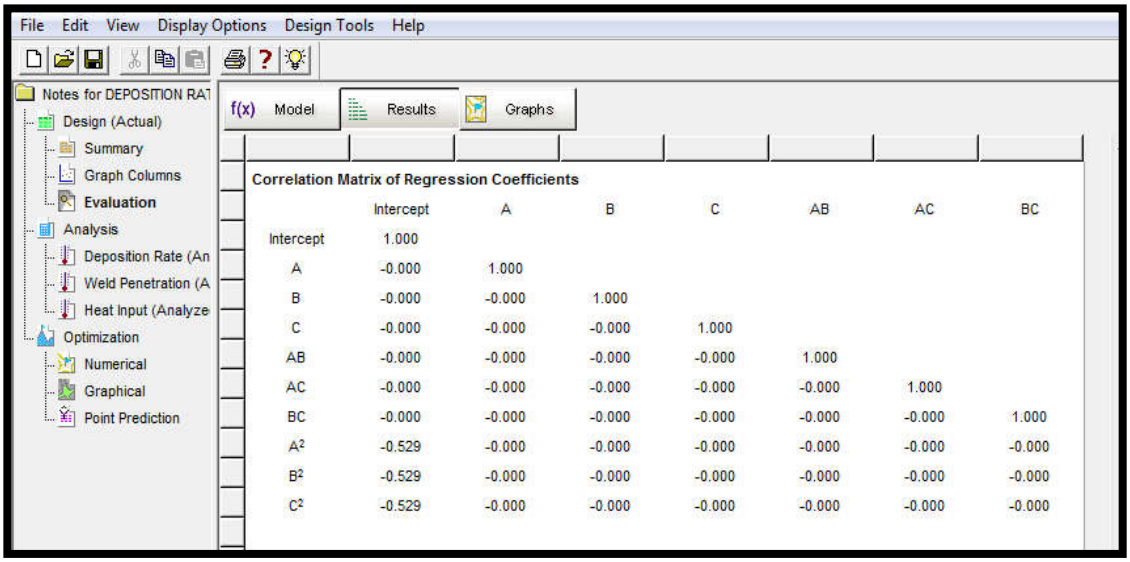

Figure 12. Correlation matrix of regression coefficients

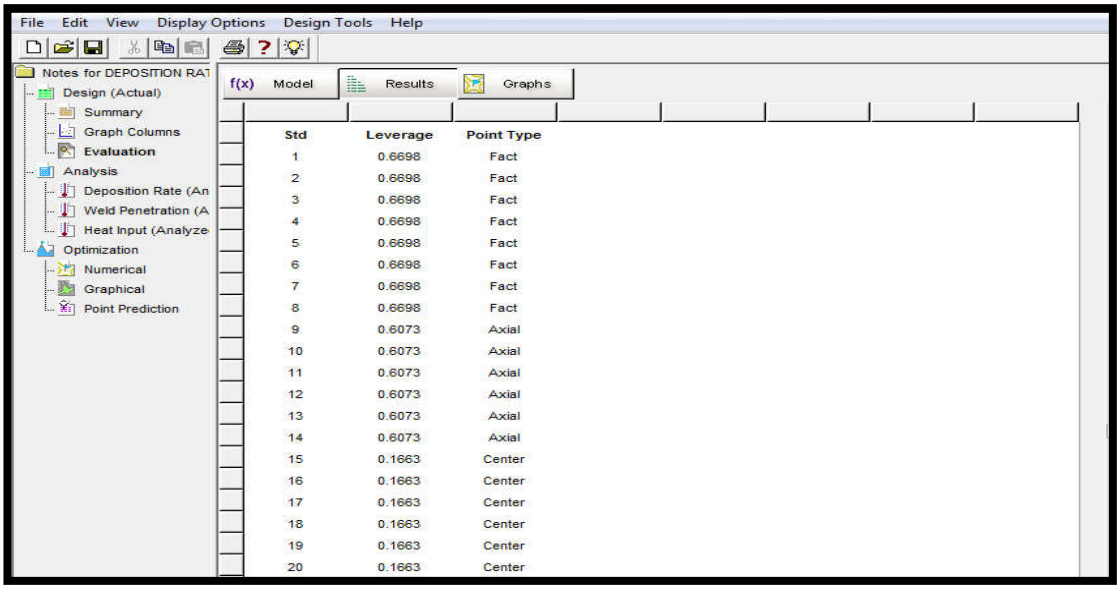

Figure 13. Computed model leverages

Lower values of the off diagonal matrix as observed in figure 12 indicates a well fitted model that is strong enough to navigate the design space and adequately optimize the selected response variables.

From the results of Figure 12, it was observed that the off diagonal matrix had coefficients that were approximately 0.00 which is an indication that the quadratic model was the ideal one for this analysis since off diagonal matrix greater than 0.00

is cause for alarm indicating a model having coefficients that are poorly correlated. To understand the influence of the individual design points on the model's predicted value, the model leveages were computed as presented in Figure 13. Leverage of a point varies from 0 to 1 and indicates how much an individual design point influences the model's predicted values. A leverage of 1 means the predicted value at that particular case will exactly equal the observed value of the experiment, i.e., the residual will be 0. The sum of leverage values across all cases equals the number of coefficients (including the constant) fit by the model. The maximum leverage an experiment can have is 1/k, where k is the number of times the experiment was replicated. Leverages of 0.6698 and 0.6073 calculated for both the factorial and axial points coupled with 0.1663 for the center point as observed in figure 13 shows that the predicted values are close to the experimental values. Hence lower residual value which shows the adequacy of the model. In assessing the strength of the quadratic model towards maximizing the deposition rate, weld penetration and optimizing the heat input, one way analysis of variance (ANOVA) was generated for the heat input response is presented in Figure 14.

Analysis of variance (ANOVA) was needed to check whether or not the model is significant and also to evaluate the significant contributions of each individual variable, the combined and quadratic effects towards each response. To validate the adequacy of the quadratic model based on its ability to optimize the heat input, the goodness of fit statistics presented in Figure 15. From the result of figure 15 it was observed that the "Predicted R-Squared" value of 0.8128 is in reasonable agreement with the "Adj R-Squared" value of 0.9170. Adequate precision measures the signal to noise ratio. A ratio greater than 4 is desirable. The computaed ratio of 14.601 as observed indicates an adequate signal. This model can be used to navigate the design space and adequately optimize the heat input. To obtain the optimal solution, we first consider the coefficient statistics and the corresponding standard errors. The computed standard error measures the difference between the experimental terms and the corresponding predicted terms. Coefficient statistics for the heat input response variable is presented in Figures 16. Variance inflation factor (VIF) value of 1.00 for the individual and combine terms, 1.02 for the quadratic terms as observed in figure 16, indicate a significant model in which the variables

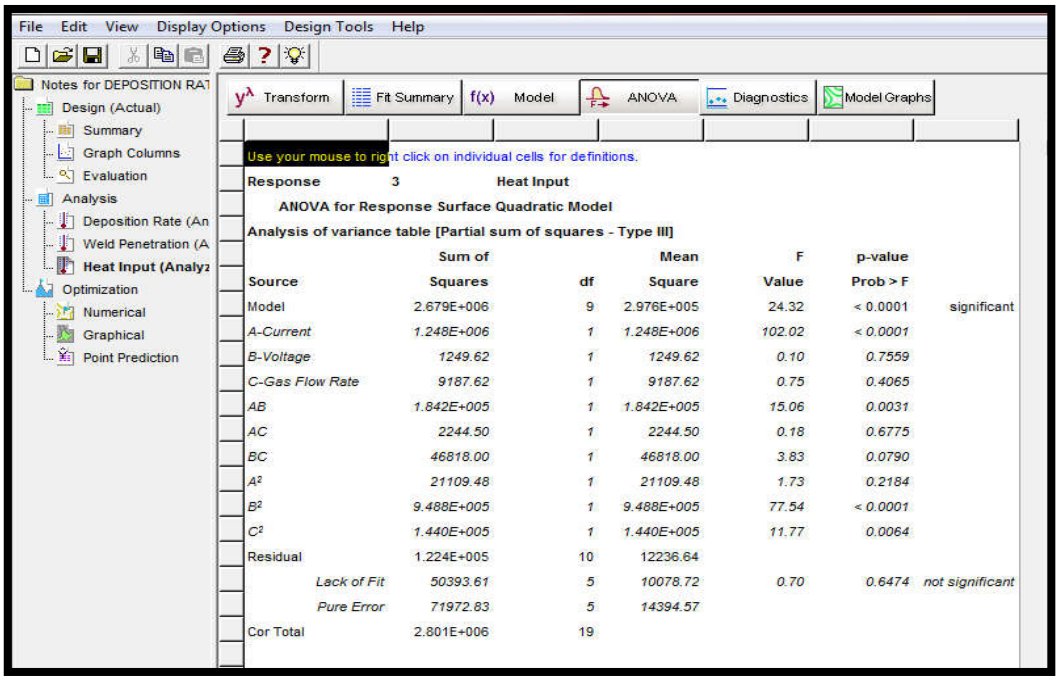

Figure 14. ANOVA table for validating the model significance towards minimizing heat input

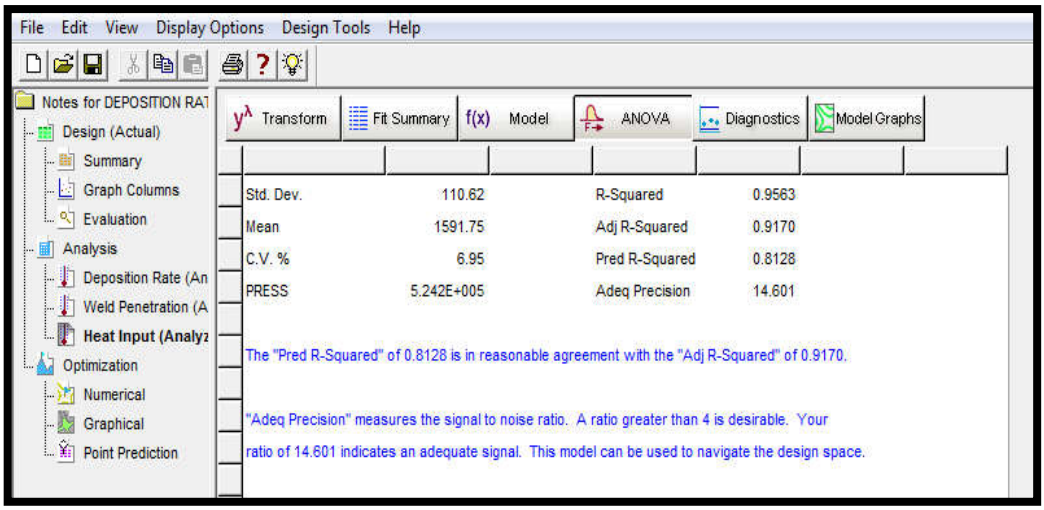

Figure 15. GOF statistics for validating model significance towards optimizing heat input

are highly correlated with the responses. The optimal equation which shows the individual effects and combine interactions of the selected input variables (current, voltage and gas flow rate) against heat input is presented based on the coded variables in Figure 17.

The optimal equation which shows the individual effects and combine interactions of the selected input variables (current, voltage and gas flow rate) against heat input is presented based on the actual factors in Figure 18.

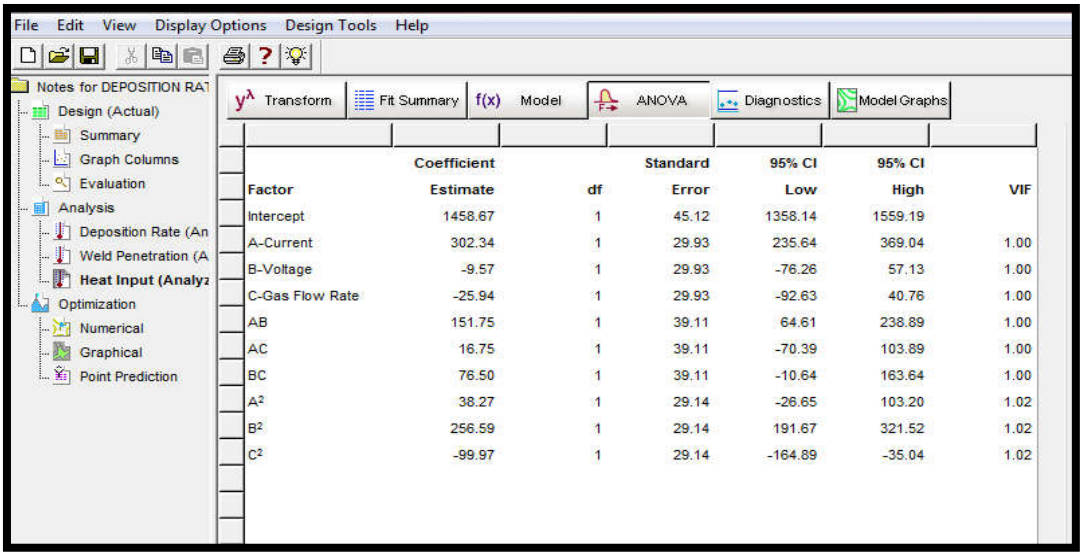

Factor	Coefficient Estimate	df	Standard Error	95% CI Low	95% CI High	VIF
Intercept	1458.67	1	45.12	1358.14	1559.19	
A-Current	302.34	1	29.93	235.64	369.04	1.00
B-Voltage	-9.57	1	29.93	-76.26	57.13	1.00
C-Gas Flow Rate	-25.94	1	29.93	-92.63	40.76	1.00
AB	151.75	1	39.11	64.61	238.89	1.00
AC	16.75	1	39.11	-70.39	103.89	1.00
BC	76.50	1	39.11	-10.64	163.64	1.00
A^2	38.27	1	29.14	-26.65	103.20	1.02
B^2	256.59	1	29.14	191.67	321.52	1.02
C^2	-99.97	1	29.14	-164.89	-35.04	1.02

Figure 16. Coefficient estimates statistics generated for optimizing heat input

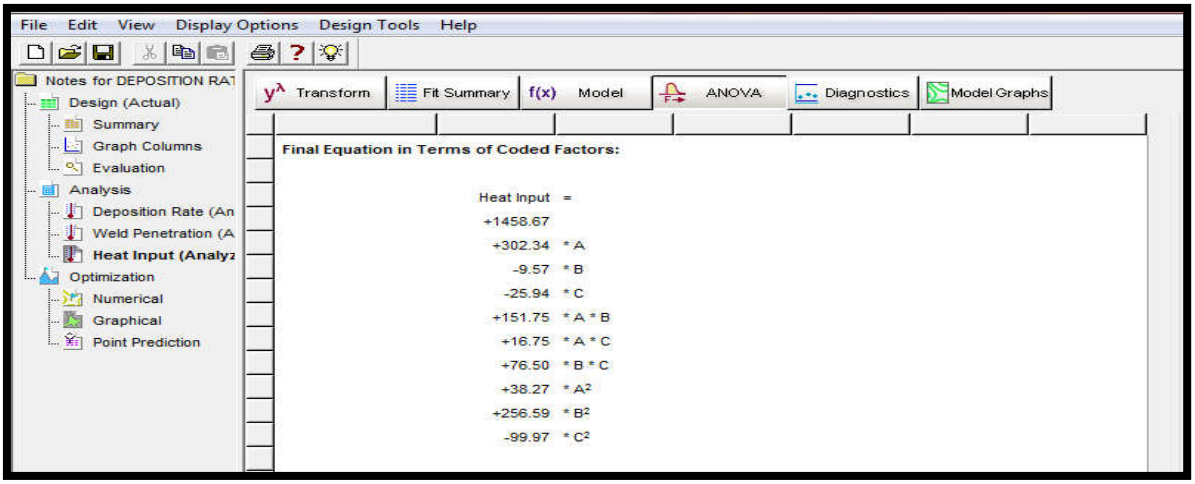

Figure 17. Optimal equation in terms of coded factors for optimizing heat input

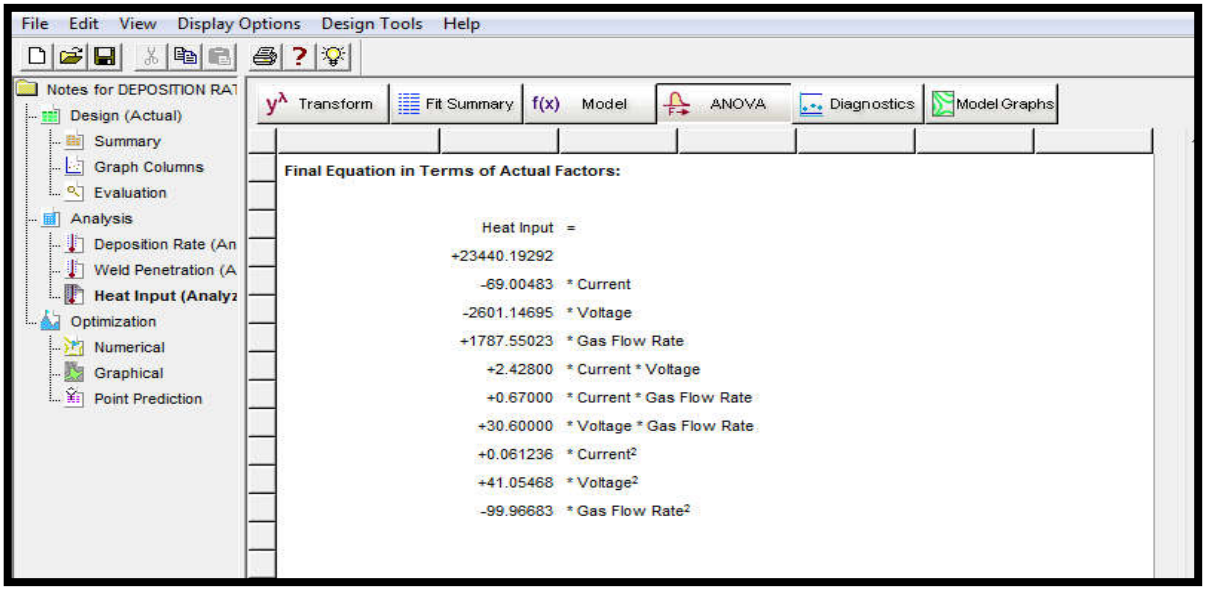

Figure 18. Optimal equation in terms of actual factors for optimizing heat input

The diagnostics case statistics which shows the observed values of heat input against their predicted values is presented in figure 19. The diagnostic case statistics actually give insight into the model strength and the adequacy of the optimal second order polynomial equation.

To asses the accuracy of prediction and established the suitability of response surface methodology using the quadratic model, a reliability plot of the observed and predicted values of heat inputdeposition rate was obtained as presented in Figures 20.

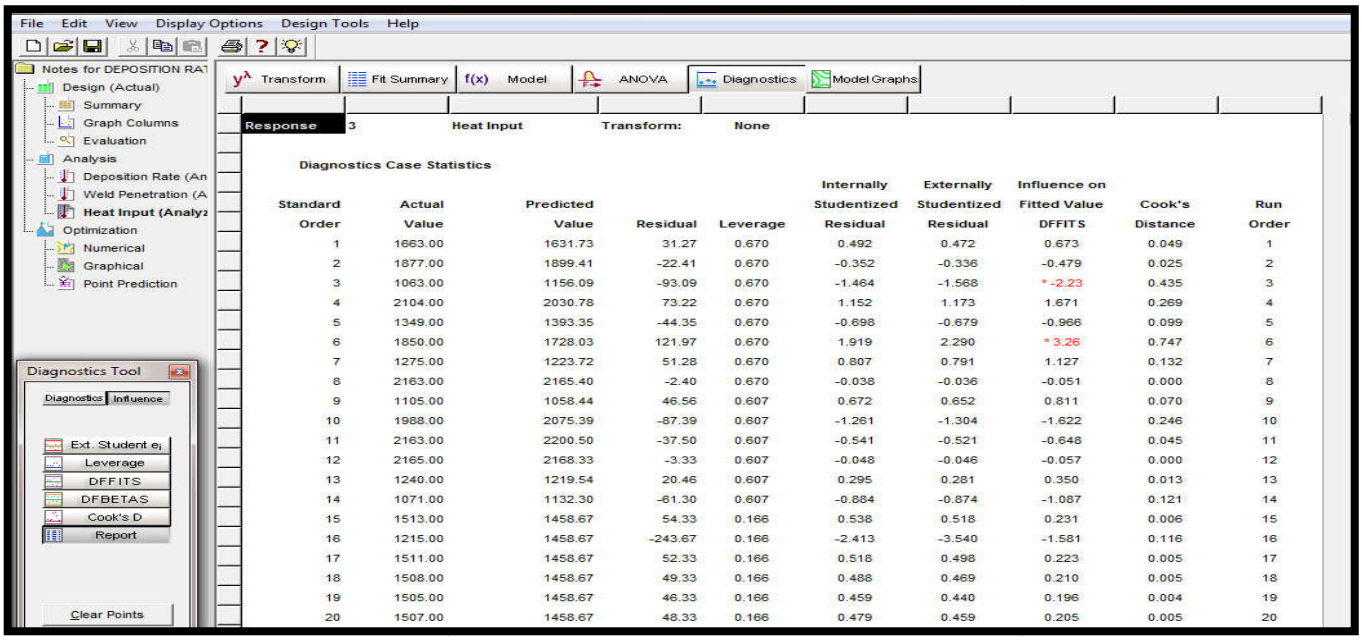

Standard Order	Actual Value	Predicted Value	Residual	Leverage	Internally Studentized Residual	Externally Studentized Residual	Influence on Fitted Value DFFITS	Cook's Distance	Run Order
1	1663.00	1631.73	31.27	0.670	0.492	0.472	0.673	0.049	1
2	1877.00	1899.41	-22.41	0.670	-0.352	-0.336	-0.479	0.025	2
3	1063.00	1156.09	-93.09	0.670	-1.464	-1.568	* -2.23	0.435	3
4	2104.00	2030.78	73.22	0.670	1.152	1.173	1.671	0.269	4
5	1349.00	1393.35	-44.35	0.670	-0.698	-0.679	-0.966	0.099	5
6	1850.00	1728.03	121.97	0.670	1.919	2.290	* 3.26	0.747	6
7	1275.00	1223.72	51.28	0.670	0.807	0.791	1.127	0.132	7
8	2163.00	2165.40	-2.40	0.670	-0.038	-0.036	-0.051	0.000	8
9	1105.00	1058.44	46.56	0.607	0.672	0.652	0.811	0.070	9
10	1988.00	2075.39	-87.39	0.607	-1.261	-1.304	-1.622	0.246	10
11	2163.00	2200.50	-37.50	0.607	-0.541	-0.521	-0.648	0.045	11
12	2165.00	2168.33	-3.33	0.607	-0.048	-0.046	-0.057	0.000	12
13	1240.00	1219.54	20.46	0.607	0.295	0.281	0.350	0.013	13
14	1071.00	1132.30	-61.30	0.607	-0.884	-0.874	-1.087	0.121	14
15	1513.00	1458.67	54.33	0.166	0.538	0.518	0.231	0.006	15
16	1215.00	1458.67	-243.67	0.166	-2.413	-3.540	-1.581	0.116	16
17	1511.00	1458.67	52.33	0.166	0.518	0.498	0.223	0.005	17
18	1508.00	1458.67	49.33	0.166	0.488	0.469	0.210	0.005	18
19	1505.00	1458.67	46.33	0.166	0.459	0.440	0.196	0.004	19
20	1507.00	1458.67	48.33	0.166	0.479	0.459	0.205	0.005	20

Figure 19. Diagnostics case statistics report of observed versus predicted heat input

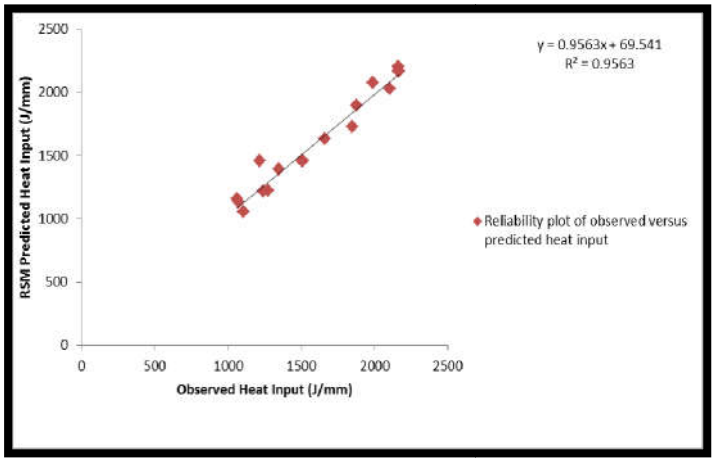

Figure 20. Reliability plot of observed versus predicted heat input

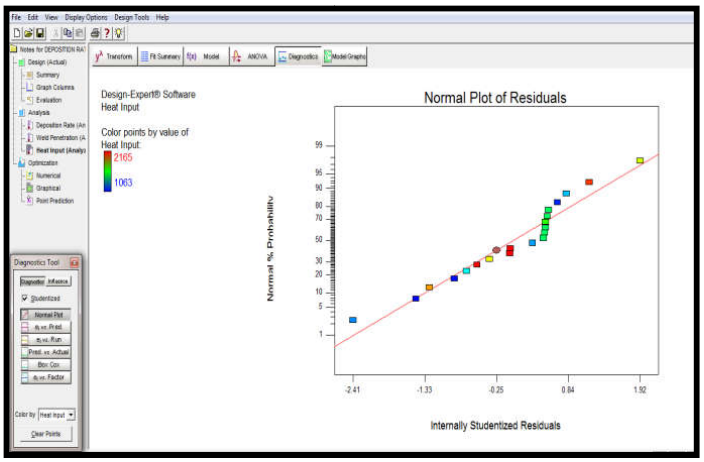

Figure 21. Normal probability plot of studentized residuals for optimizing heat input

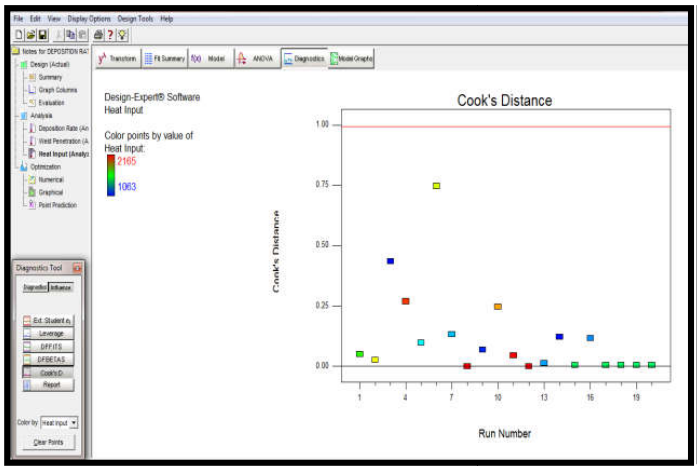

Figure 22. Generated cook's distance for heat input

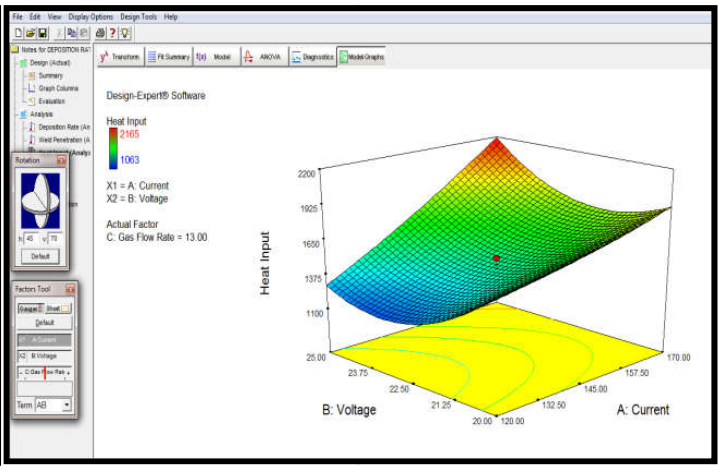

Figure 23. Effect of current and voltage on heat input

The high coefficient of determination (r^2 = 0.9739, 0.9751 and 0.9563) as observed in Figure 20 were used to established the suitability of response surface methodology in maximizing the deposition rate, weld penetration and optimizing the heat input. To accept any model, its satisfactoriness must first be checked by an appropriate statistical analysis output. To diagnose the statistical properties of the response surface model, the normal probability plot of heat input for deposition rate was presented in Figure 21. The normal probability plot of studentized residuals was employed to assess the normality of the calculated residuals. The normal probability plot of residuals which is the number of standard deviation of actual values based on the predicted values was employed to ascertain if the residuals (observed – predicted) follows a normal distribution. It is the most significant assumption for checking the sufficiency of a statistical model. Result of Figure 21 revealed that the computed residuals are approximately normally distributed an indication that the model developed is satisfactory. To determine the presence of a possible outlier in the experimental data, the cook's distance plot was generated for the different responses.

The cook's distance is a measure of how much the regression would change if the outlier is omitted from the analysis. A point that has a very high distance value relative to the other points may be an outlier and should be investigated. The generated cook's distance for heatinput is presented in Figures 22. The cook's distance plot has an upper bound of 1.00 and a lower bound of 0.00. Experimental values smaller than the lower bound or greater than the upper bounds are considered as outliers and must be properly investigated. Results of Figure22 indicates that the data used for this analysis are devoid of possible outliers thus revealing the adequacy of the experimental data. To study the effects of combine input variables on heat input response variable, 3D surface plots showing the topography of the response is presented in Figure 23. The 3D surface plot as observed in Figure 23 shows the relationship between the input variables (current and voltage) against the response variables (deposition rate, weld penetration and heat input) It is a 3 dimensional surface plot which was employed to give a clearer concept of the response surface.

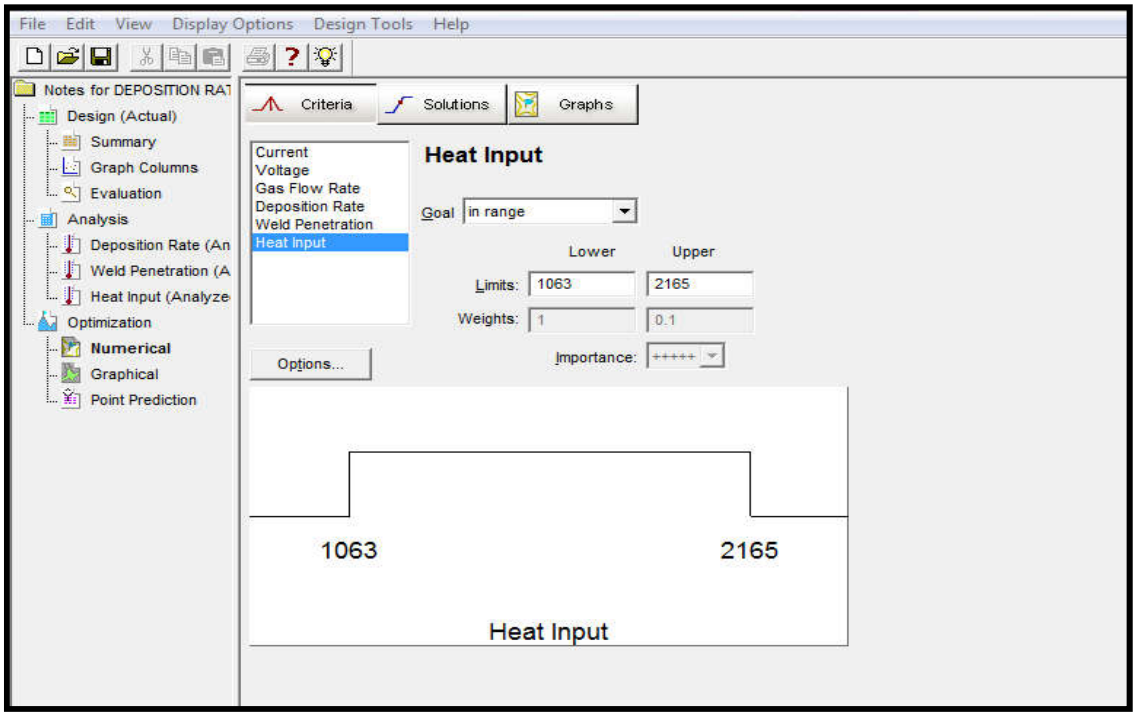

Figure 24. Interphase of numerical optimization model for optimizing heat input

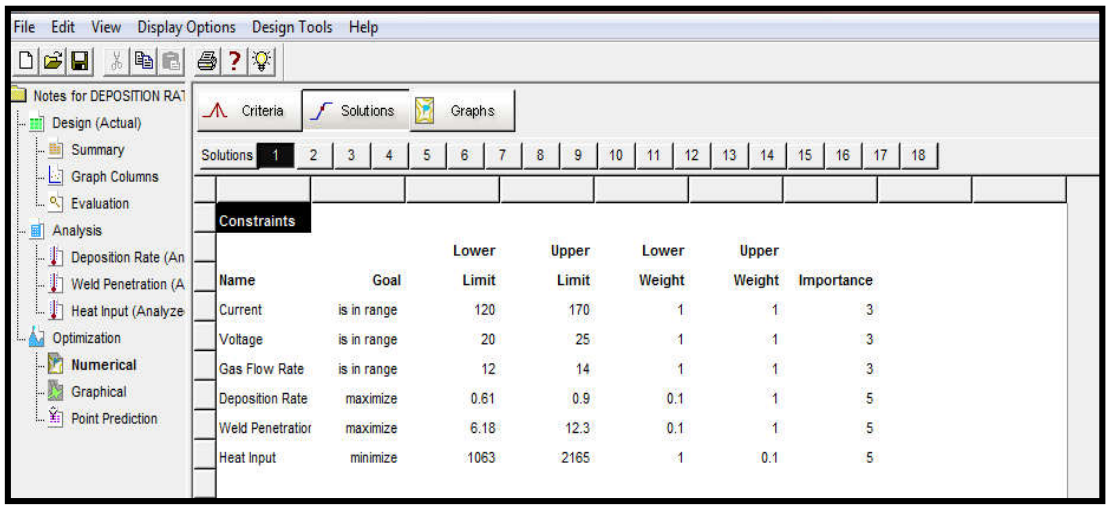

Figure 25. Constraints for numerical optimization of selected responses

Although not as useful as the contour plot for establishing responses values and coordinates, this view may provide a clearer picture of the surface. As the colour of the curved surface gets darker, the deposition rate and weld penetration increase proportionately while the heat input decreases. The presence of a coloured hole at the middle of the upper surface gave a clue that more points lightly shaded for easier identification fell below the surface. In Figure 23, it was observed that the colour of the surface gets dark towards the current and voltage and indication that increasing current and voltage will bring about a corresponding increase in heat input

Finally, numerical optimization was performed to ascertain the desirability of the overall model. In numerical optimization phase, we ask design expert to optimizing the heat input. In addition, the optimum current, voltage and gas flow rate was determined simultaneously. The interphase of the numerical optimization showing the objective function is presented in Figure 24.

The constraint set for the numerical optimization algorithm is presented in Figure 25. The numerical optimization produces about eighteen (18) optimal solutions which are presented in Figure 26. From the results of figure 26, it was observed that a current of 120amp, voltage of 20volt, and gas flow rate of 12.00 L/min will result in a welding process with weld penetration of 10.775mm. This solution was selected by design expert as the optimal solution with a desirability value of 98.80%. The ramp solution which is the graphical presentation of the optimal solution is presented in Figure 27. While the desirability bar graph which shows the accuracy with which the model is able to predict the values of the selected input variables and the corresponding responses is shown in Figure 28. It can be deduce from the result of Figure 28 that the model developed based on response surface methodology and optimized using numerical optimization method, predicted the deposition rate by an accuracy level of 99.98%, weld penetration by an accuracy level of 97.17% and heat input by

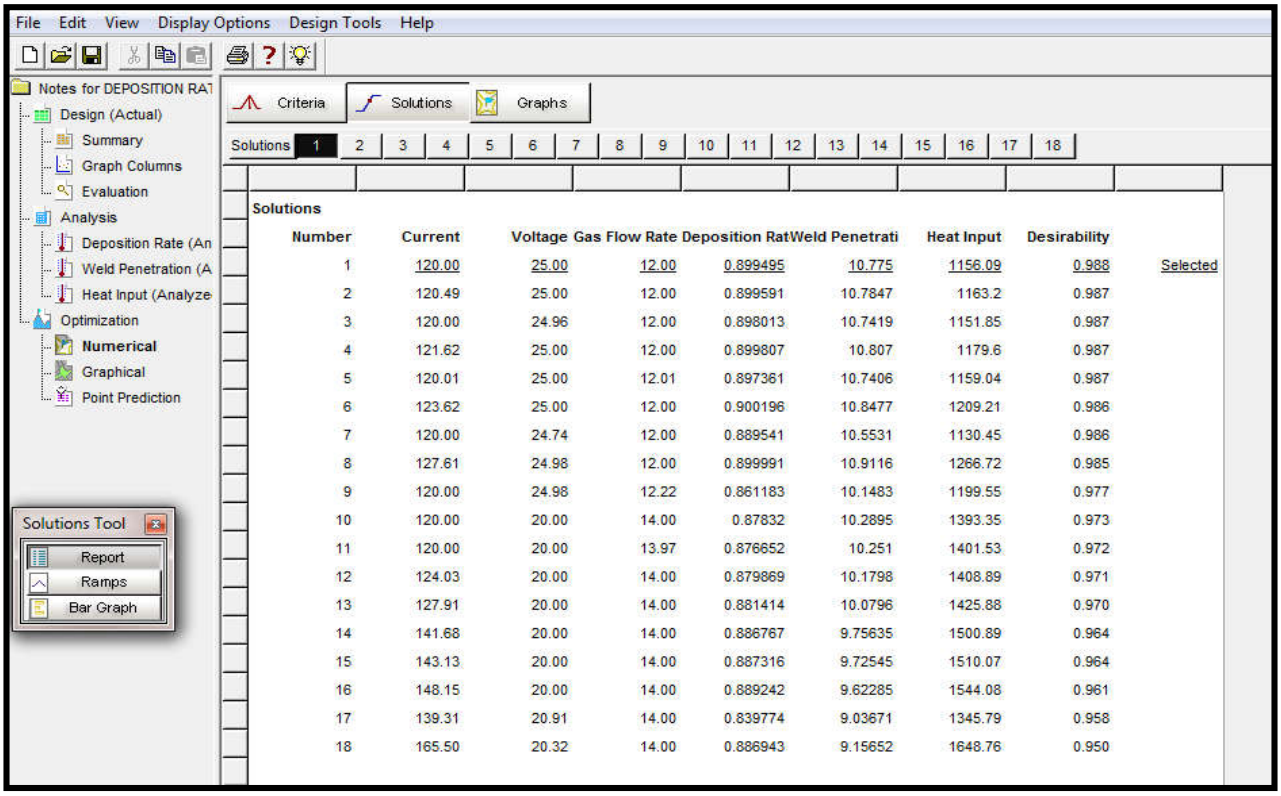

Solutions

Number	Current	Voltage	Gas Flow Rate	Deposition Rat	Weld Penetrati	Heat Input	Desirability	
1	120.00	25.00	12.00	0.899495	10.775	1156.09	0.988	Selected
2	120.49	25.00	12.00	0.899591	10.7847	1163.2	0.987	
3	120.00	24.96	12.00	0.898013	10.7419	1151.85	0.987	
4	121.62	25.00	12.00	0.899807	10.807	1179.6	0.987	
5	120.01	25.00	12.01	0.897361	10.7406	1159.04	0.987	
6	123.62	25.00	12.00	0.900196	10.8477	1209.21	0.986	
7	120.00	24.74	12.00	0.889541	10.5531	1130.45	0.986	
8	127.61	24.98	12.00	0.899991	10.9116	1266.72	0.985	
9	120.00	24.98	12.22	0.861183	10.1483	1199.55	0.977	
10	120.00	20.00	14.00	0.87832	10.2895	1393.35	0.973	
11	120.00	20.00	13.97	0.876652	10.251	1401.53	0.972	
12	124.03	20.00	14.00	0.879869	10.1798	1408.89	0.971	
13	127.91	20.00	14.00	0.881414	10.0796	1425.88	0.970	
14	141.68	20.00	14.00	0.886767	9.75635	1500.89	0.964	
15	143.13	20.00	14.00	0.887316	9.72545	1510.07	0.964	
16	148.15	20.00	14.00	0.889242	9.62285	1544.08	0.961	
17	139.31	20.91	14.00	0.839774	9.03671	1345.79	0.958	
18	165.50	20.32	14.00	0.886943	9.15652	1648.76	0.950	

Figure 26. Optimal solutions of numerical optimization model

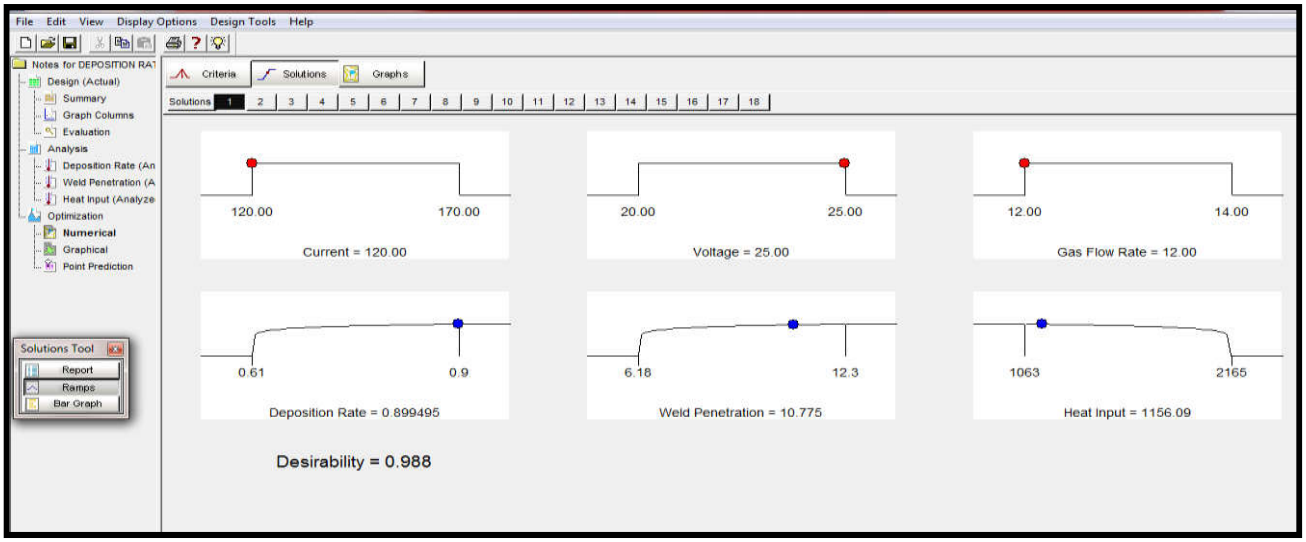

Figure 27. Ramp solution of numerical optimization

an accuracy level of 99.12%. Finally, based on the optimal solution, the contour plots showing heat input response variable against the optimized value of the input variable is presented in Figure 29 based on the optimal solution, the contour plots showing desiribility response variable against the optimized value of the input variable is presented in Figure 30. As presented in Figure 30, the contour plot can be employed to predict the optimum values of the input variables based on the flagged response variables.

Figure 28. Prediction accuracy of numerical optimzation

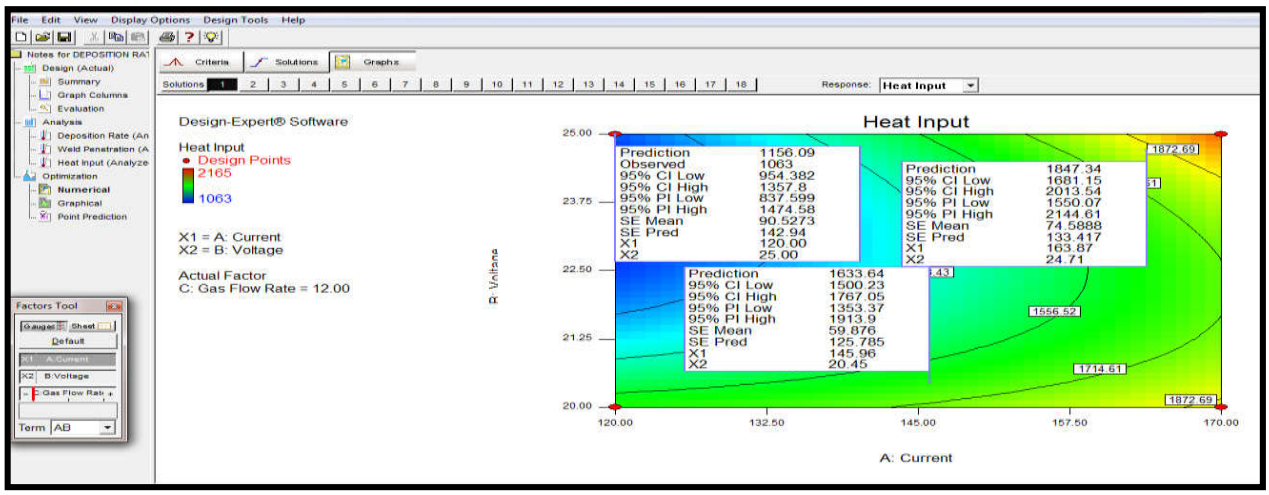

Figure 29. Predicting heat input using contour plot

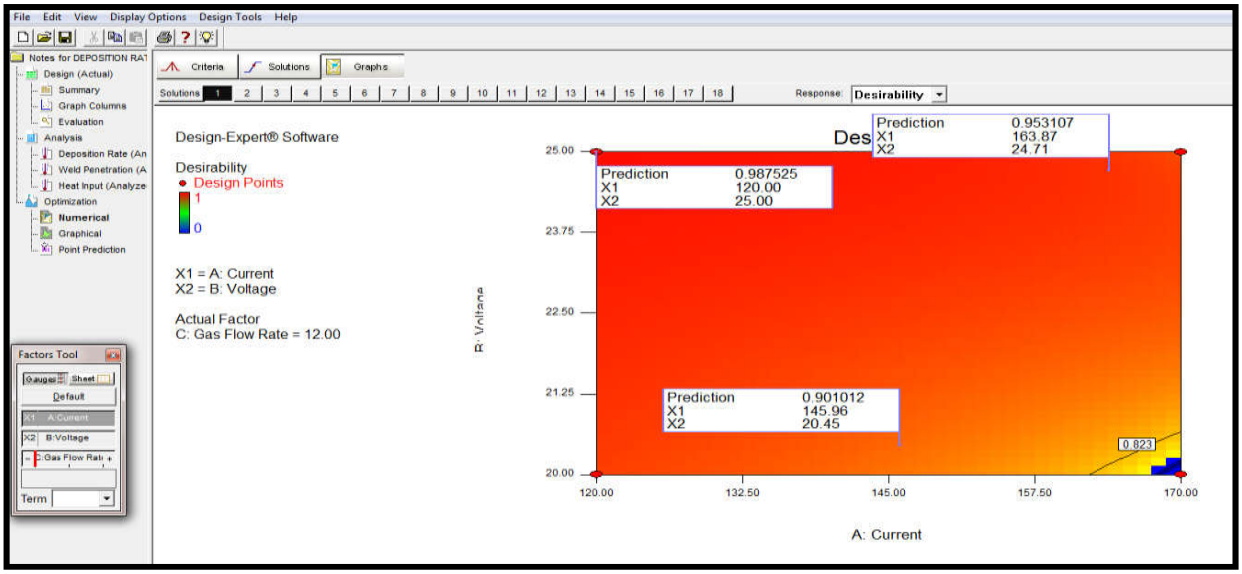

Figure 30. Predicting desirability using contour plot

Findings

From the study, the following are the findings:

- Results of the sequential sum of square , revealed that the quadratic model is suitable to model the experimental data collected from the experiment
- The cookes distance plot revealed that the data all clustered around the mean ,indicating that the RSM model is fit for analyzing this data
- From the numerical optimization results it was observed that a current current of 120amp, voltage of 20volt, and gas flow rate of 12.00 L/min will result in a welding process with Heat Input of 1156.09J/mm

Conclusion

The quality of a weld can be determined by the size of the weld penetration, deposition rate and heat input. In this study the response, surface methodology was employed to predict and optimize the responses stated above. The results obtained shows that the voltage has very strong influence on the heat input. The models developed possess a variance inflation factor of 1 and P- values < 0.05 indicating that the models are significant, the models also possessed a high goodness of fit with R^2 (Coefficient of determination) values of 95.9% for WDR, 95.1% for heat input and 92.3% for weld penetration respectively The reasonable agreement between the predicted R^2 value and the adjusted- R^2 value was employed as a bases to justify the adequacy of the second order polynomial equation and the suitability of RSM in creating a better explanation to the experimental data.. The noise to signal ratios were greater than 4, which indicates that the models have adequate strength and potency to predict its target response.

REFERENCES

Apurv, C., and Vijaykumar, J. S. 2014. “Influence of Heat Input on Mechanical Properties and Microstructure of Austenitic 202 grade Stainless Steel Weldments” WSEAS transactions on applied and theoretical mechanic Volume 9, 2014.

Correia, D.S., Gonçalves, C.V., Da Cunha, S.S., and Ferraresi, V.A. 2005. "Comparison between Genetic Algorithms and Response Surface Methodology in GMAW Welding Optimization", *Journal of Materials Processing Technology* Vol. 160, No. 1, 70-76.

Doniavi, A., Hosseini, A., and Ranjbary, G. 2016. “Prediction and Optimization of Mechanical Properties of St52 in Gas Metal Arc Weld Using Response Surface Methodology and ANOVA”, *International Journal of Engineering Transaction C: Aspects* vol. 29, No. 9 pp 1307 – 1313.

Deshmukh A.R., G.Venkatachalam, Hemant Divekar, M.R.Saraf (2014), Effect of Weld Penetration on Fatigue Life. Elsevier. Procedia Engineering. Volume 97, 2014, Pages 783-789. https://doi.org/10.1016/j.proeng. 2014.12.277

Hari, O.M., and Sunil, P. 2013. ”Effect of heat input on dilution and heat affected zone in submerged arc welding process” Indian Academy of Sciences Vol. 38, Part 6, December 2013, pp. 1369–1391.

Honggang, D., Xiaohu, H., and Dewei, D. 2014. “Effect of Welding Heat Input on Microstructure and Mechanical Properties of HSLA Steel Joint”, Metallogr. Microstruct. Anal. (2014) 3:138–146

Hu, J., DU, L., Wang, J., and Gao, C. 2013. “Effect of Welding heat input on microstructures and toughness in Simulated CGHAZ of V-N high strength steel”, Materials Science and Engineering A, 577, pp. 161 – 168.

Kim, D. and Rhee, S., 2001, “Optimization of Arc Welding Process Parameters using a Genetic Algorithm”, Welding Journal, July, pp. 184-189.

Myers, R. H. and Montgomery, D. H., 1995, “Response Surface Methodology”, John Wiley & Sons, USA, 705p

Popovic, O., Prokic-Cvetkovic, R., Burzic, M. and Milutinovic, Z. 2010. The Effect of Heat Input on the Weld Metal Toughness of Surface Welded Joint. 14th International Research/Expert Conference “Treads in the Development of Machinery and Associated Technology”. TMT 2010, Mediterranean Cruise, 11 – 18 September 2010.

Suneel, R.J. and Jagadeesh, P.G. 2016. Simultaneous optimization of multiple quality characteristics in TIG welding of AA5083; H111 Aluminum Alloy using Response Surface Methodology coupled with composite desirability function. *International journal of applied engineering research*., ISSN 00973 – 4562. Vol. 11 pp 6525 – 6541

****